SIMULATION OF ULTRA-HIGH-PERFORMANCE DENSE CONCRETE WITH SAND, BARITE AND MAGNETITE ON MECHANICAL AND RADIATION SHIELDING AS DRY CASK STORAGE OF SPENT NUCLEAR FUEL

M.A.H. Abdullah[1,2,*], Raizal S.M. Rashid[1], N.M. Azreen[5] H. Ithnin[5], Y.L. Voo[6], M.I. Idris[7]

[1]*Department of Civil Engineering, Faculty of Engineering, Universiti Putra Malaysia, 43400 Serdang, Selangor, Malaysia*

[2]*Department of Civil Engineering Technology, Faculty of Civil Eng. and Tech.,University Malaysia Perlis, 02100 Perlis, Malaysia*

[5]*Industrial Technology Division, Malaysia Nuclear Agency, 43600 Kajang, Selangor, Malaysia*

[6]*DURA Technology Sdn. Bhd, Jalan Chepor 11/8, Pusat Seramik Fasa 2, Ulu Chepor, 31200 Chemor, Perak, Malaysia*

[7]*School of Applied Physics, Faculty of Science and Technology, National University of Malaysia, 43600 Selangor, Malaysia*

**Corresponding author: afiqhizami@unimap.edu.my*

ABSTRACT

Harnessing of nuclear energy provides lots of benefits in healthcare, power generation and advancement in agriculture but the penetrative nature of its energy requires shielding which has been vastly made of concrete due to its ubiquitous components and durability. This study aimed to investigate the performance of UHPC with colemanite and polyvinyl alcohol (PVA) fibre in term of mechanical, radiation shielding that includes neutron shielding by method of computer simulation. This type of modified UHPC is denoted as ultra-high performance dense concrete (UHPdC) and the simulations are carried out using ANSYS and Particle and Heavy Ion Transport code System (PHITS) are carried out to validate the experimental data and evaluate UHPdC's performance as dry cask storage for spent fuel cell.

ABSTRAK

Memanfaatkan tenaga nuklear memberikan banyak faedah dalam penjagaan kesihatan, penjanaan kuasa dan kemajuan dalam pertanian tetapi sifat penembusan tenaganya memerlukan perisai yang kebanyakannya diperbuat daripada konkrit kerana komponennya yang ada di mana-mana dan ketahanan. Kajian ini bertujuan untuk mengkaji prestasi UHPC dengan gentian colemanite dan polivinil alkohol (PVA) dari segi mekanikal, perisai sinaran yang merangkumi perisai neutron melalui kaedah simulasi komputer. Jenis UHPC yang diubah suai ini ditandakan sebagai konkrit padat prestasi ultra tinggi (UHPdC) dan simulasi dijalankan menggunakan ANSYS dan Sistem Kod Pengangkutan Zarah dan Ion Berat (PHITS) dijalankan untuk mengesahkan data eksperimen dan menilai prestasi UHPdC sebagai kering. simpanan tong untuk sel bahan api terpakai.

Keywords: simulation ANSYS, concrete, spent nuclear fuel, shielding material

INTRODUCTION

Harnessing of nuclear energy provides lots of benefits in healthcare, power generation and advancement in agriculture but the penetrative nature of its energy requires shielding which has been vastly made of concrete due to its ubiquitous components and durabiity [1]–[5]. Familiarity of concrete as shielding for radiation is indicated by research that improves its radiation shielding properties via incorporation of beneficial element [6]–[8]. Even though recent research investigated the viability of adopting recycle and sustainable sources as component in radiation shielding concrete, natural occurring heavyweight aggregate produced concrete with better gamma radiation shielding while natural mineral containing neutron absorber improves concrete's neutron shielding property [9], [10]. However, replacement of sand; which commonly used in concrete, with heavyweight aggregate such as barite resulted in lower compressive strength but not with magnetite **[6], [11].** However, a study on barite concrete shows better strength with incorporation of nano filler which opens up wider field of investigation [12]. Rather than heavyweight filler, neutron absorbing filler such as colemanite would improve concrete's neutron shielding property yet current research indicate that presence of colemanite in barite concrete resulted in lower compressive strength due to weak adhesion between hydrated cement and colemanite [13]. Vast study on radiation shielding concrete have been conducted but there is a dearth of data involving ultra-performance concrete as most of the research produced concrete with compressive and tensile strength of 49 MPa and 3 MPa [14]–[16]. Study also shows radiation shielding concrete possess low durability based on large mass loss due to sulfate attack [17]. Furthermore, thermal durability of radiation shielding concrete is low based on 30 and 90 % loss of strength and neutron shielding respectively when exposed to 500 °C [18]. Further increase in temperature of 800 °C resulted in 84.8 % of loss in compressive strength [19]. Utilization of ultra-high performance concrete (UHPC) which possess compressive strength of more than 120 MPa with superior thermal durability due to incorporation of fibre would provide nuclear related facility with better shielding [20]–[24]. Few research on UHPC as radiation shielding material shows compressive and flexural strength of more than 138 and 20 MPa respectively [7], [25], [26]. A research on magnetite UHPC shows residual compressive strength of 23 MPa after exposure to 800 °C [27]. However, there is lack of works on other type of heavyweight aggregate and incorporation with neutron absorbing mineral. Furthermore, there is also dearth of study on UHPC's neutron shielding performance which is beneficial for wider application in nuclear related facility. Hence, this study aimed to investigate the performance of UHPC with colemanite and polyvinyl alcohol (PVA) fibre in term of mechanical, radiation shielding that includes neutron shielding by method of computer simulation. This type of modified UHPC is denoted as ultra-high performance dense concrete (UHPdC) and the simulations are carried out using ANSYS and Particle and Heavy Ion Transport code System (PHITS) are carried out to validate the experimental data and evaluate UHPdC's performance as dry cask storage for spent fuel cell.

SIMULATION WORK

Structural simulation on beam and dry cask storage

Structural simulations are carried out using ANSYS to validate the flexural data of the experimental work. Beam sample of same dimension are simulated with flexural modulus that is calculated using the Equation 1 as listed in ASTM D790:

$$E_B = \frac{L^3 m}{4bd^3} \qquad \textbf{(Eq. 1)}$$

where E_B is the modulus of elasticity in bending in MPa, L is the distance between support in mm, b is the breadth of the beam in mm, d is the depth of the beam in mm and m is the slope of the initial straight line in the load-deflection curve (N/mm).

Experimental work is validated by comparing the value of deflection calculated in the simulation and recorded in the experimental work.

Simulation of dry cask storage is carried out using data of compressive strength each UHPdC with capacity to sustain self-weight due to stacking of the cask. Modulus of elasticity is calculated using Equation 2 as suggested by [32];

$$E_c = 4069\sqrt{f'_c} \quad \textbf{(Eq. 2)}$$

where E_c is the modulus of elasticity in MPa and f'$_c$ is the compressive strength.

Based on E_c, simulation is carried out based on dimension used in research on radiation shielding of dry cask storage [33]. Table 1 shows the detail dimension of the cask.

Table 1: Dimension of concrete dry cask storage based on previous research [33]

Height (mm)	5240
Inner diameter (mm)	2240
Outer diameter (mm)	2890
Wall thickness (mm)	325

Radiation Shielding Simulation on Dry Cask Storage

Radiation shielding simulation is carried out using PHITS and the dry cask model is based on similar dimension used in structural simulation. Based on this dimension, model is developed as two nested right circular cylinder macrobodies. Material defined for the cask is based on density, XRF analysis and composition of each type of UHPdC. Two type of source which are based on previous work that are photon and neutron [33]. Source is set as isotropic point source at 2620 mm from base of the cask along the axis. A maximum of 10,000 numbers of source particle history is defined which produced an acceptable relative error. Flux value from the simulation is converted into dose rate based on coefficient of International Commission on Radiological Protection (ICRP) 74.

Experimental Data

Experimental data of UHPdC consist of three types of UHPdC namely sand UHPdC, barite UHPdC and magnetite UHPdC. The composition of these UHPdCs are shown in

Table 2. Sample in triplicate of each type of UHPdC are then tested for compressive strength, residual compressive strength after heating at 800 °C, flexural strength test and splitting tensile strength test which are in accordance to BS EN 12390-3, BS EN 12390-5 and BS EN 12390-6. Samples are also tested for shielding against gamma and neutron radiation. Gamma radiation is sourced from Cs-137 and Co-60 while neutron radiation is sourced from AmBe. The summary of experimental results are shown in Table 3.

Table 2: Mix design for UHPdC

Sample	**Cement (kg/m^3)**	**Silica Fume (kg/m^3)**	**Sand/Barite/Magnetite (kg/m^3)**	**Colemanite (kg/m^3)**	**PVA (kg/m^3)**	**Super plasticizer (kg/m^3)**	**Steel Fibres (kg/m^3)**	**Water (kg/m^3)**
Sand UHPdC	825	200	950	50	9.75	28	120	191
Barite UHPdC	825	200	1580	50	9.75	28	120	226

Magnetite UHPdC	825	200	1819	50	9.75	28	120	236

Table 3: Experimental data of UHPdC

	Compressive Strength (MPa)	Residual Compressive Strength (MPa)	Flexural Strength (MPa)	Splitting Tensile Strength (MPa)	Linear Attenuation Coefficient against Cs-137 (cm^{-1})	Linear Attenuation Coefficient against Co-60 (cm^{-1})	Macroscopic Removal Cross Section against AmBe (cm^{-1})
Sand UHPdC	131	30.69	20.05	17.55	0.1663	0.1156	0.0262
Barite UHPdC	116	30.21	14.05	14.39	0.1957	0.1306	0.027
Magnetite UHPdC	119	49.42	17.01	15.18	0.1972	0.139	0.0307

RESULTS AND DISCUSSION

Structural simulation using ANSYS

Simulations are carried out using ANSYS software and modelled on flexural tests that were carried out on UHPdC of sand, barite and magnetite. Based on the calculated flexural modulus and peak load recorded for each sample, model of beam is simulated to produce displacement on z-axis as point of validation. Overall, simulated deflection is lower compared to experimental data but at only small amount. Experimental data recorded 5 mm deflection at peak load while simulated deflection for sand UHPdC is 4.52 mm (Figure 1). While barite and magnetite UHPdC recorded 4.46 and 4.51 mm simulated deflection. Summary of data is shown in Table 4 and it can be summarized that the results of simulation validated the experimental results.

Table 4: Summarized data on samples simulated in ANSYS

Sample	Flexural modulus (GPa)	Peak load (kN)	Deflection – Experimental (mm)	Deflection – simulation (mm)
Unoptimized sand UHPC	1.61	50.4	5	4.52
Optimized sand UHPdC	1.60	50.1	5	4.52
Optimized barite UHPdC	1.12	35.1	5	4.46
Optimized magnetite UHPdC	1.36	42.5	5	4.51

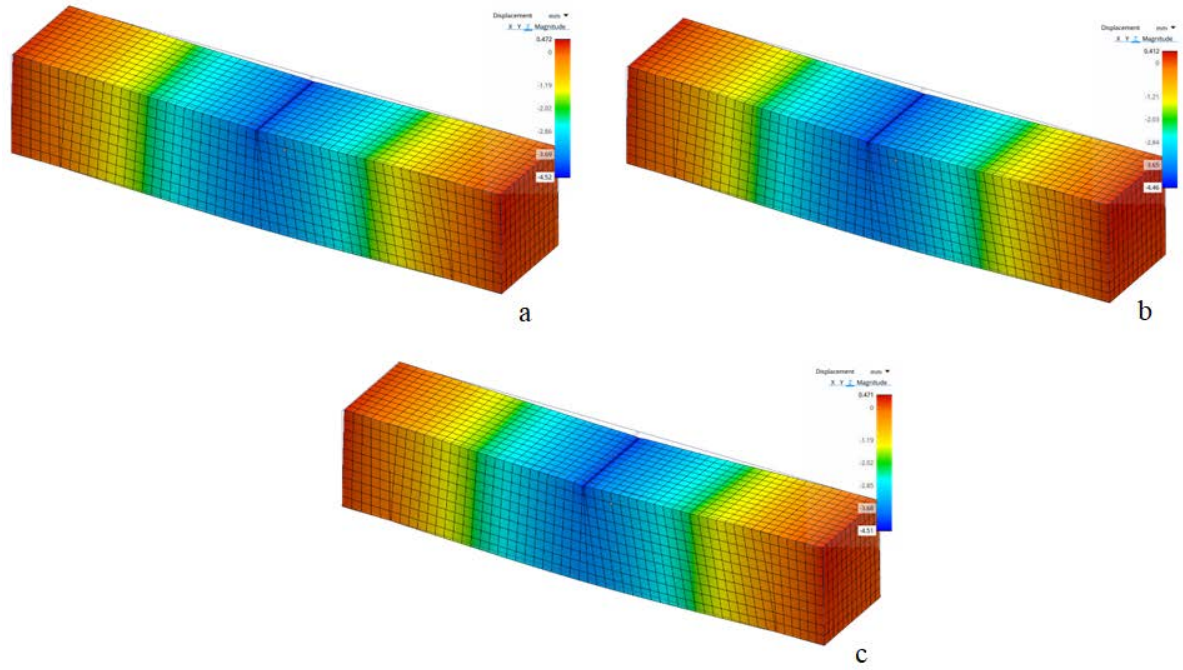

Figure 1: Simulated beam deflection of (a) sand UHPdC, (b) barite UHPdC and (c) magnetite UHPdC

Further simulation on application of UHPdC as dry cask storage is carried out based on dimension from previous work which follows Nuclear Regulatory Commission on spent fuel storage and handling [33] (Figure 2). Structural simulation is design with stacking loading of another dry cask storage to maximise usage per area. Modulus of elasticity is calculated using Equation 4 based compressive strength results of the experimental work. Based on the simulations, UHPdCs shows no significant deformation due stacking loading. Maximum deformation of 0.0381, 0.0467 and 0.0498 mm is recorded by sand, barite and magnetite UHPdC respectively (Figure 3). However, deformations recorded by barite and magnetite UHPdC is larger due to their denser property which resulted in larger axial loading when stacked.

Overall, UHPdC is viable to be applied as dry cask storage that follows guideline by the regulatory commission. Furthermore, simulation on the cask to withstand stacking load would increase the storage per area.

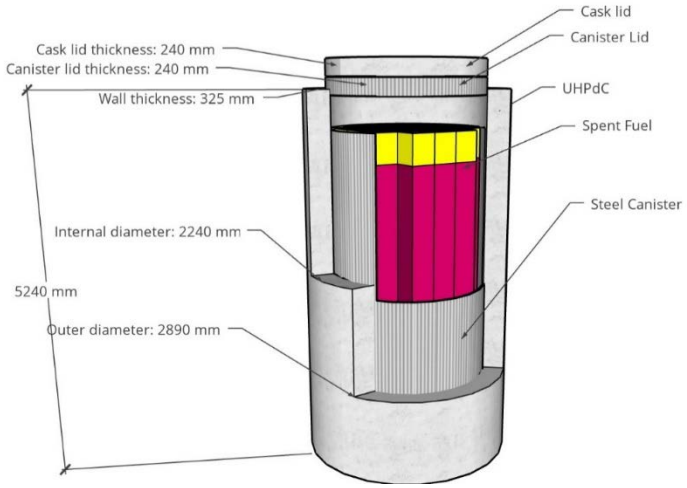

Figure 2: Reproduced 3d model of dry cask storage from [33]

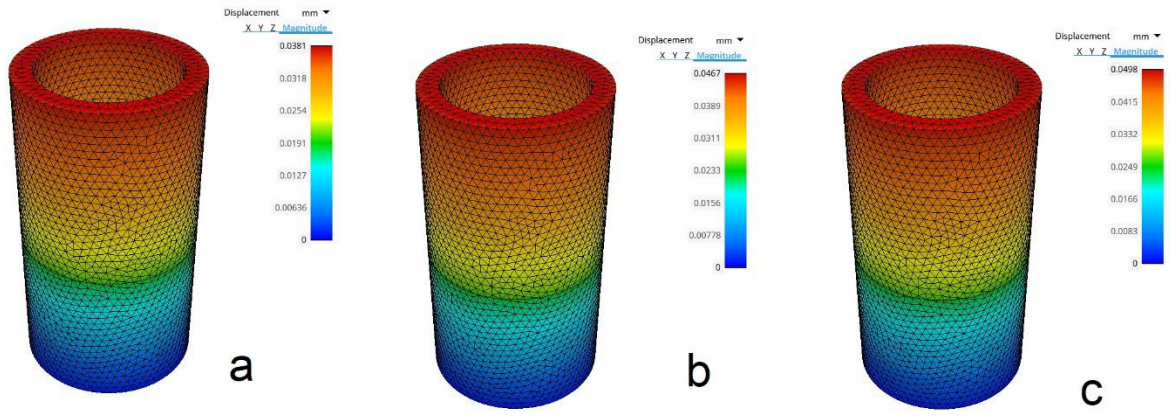

Figure 3: Simulated dry cask storage of a. sand UHPdC, b. barite UHPdC and magnetite UHPdC

Radiation shielding simulated using PHITS

The dry cask storage model used in ANSYS is also simulated for radiation shielding using PHITS software which is a particle transport simulation software using Monte Carlo. Dry cask dimension is defined in geometry section while observation and tracking of particles are defined in tally section. T-track is defined for tally parameter which record the transport of particle within the area of interest. Total of 10000 histories per batch and a total of 10 batches are defined in the simulation to achieve acceptable statistical error.

Figure 4 shows result of simulation on quadrant section of UHPdC dry cask storages. The results show the flux intensity tracked from center of cask up to 200 cm radius. Intensity of flux increase as the colour changes from blue to red. The red dot shown in each quadrant indicates the location of source and the colour changes to yellow and teal up to perimeter of dry cask wall. Furthermore, all quadrant shows blue colour in the region outside of dry cask storage which indicates that all UHPdCs dry cask are able to contain the gamma radiation.

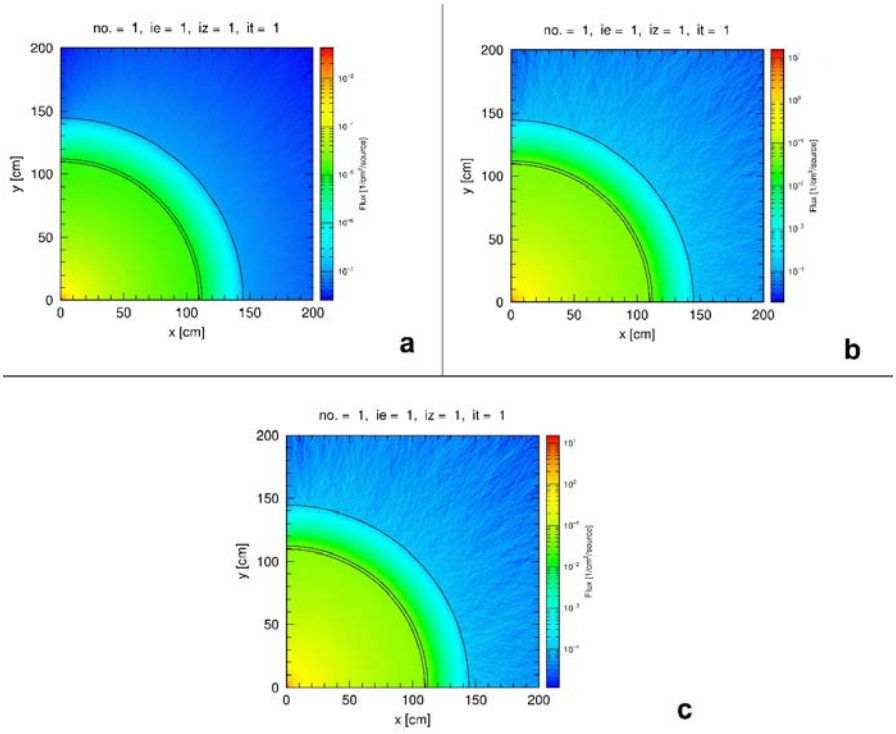

Figure 4: Gamma ray shielding simulated result of dry cask storage using a. sand UHPdC, b. barite UHPdC and c. magnetite UHPdC

Deeper analysis based on effective dose shown by Figure 5 indicates sharp declines in dose value from the inside wall towards the outside face of dry cask. Highest dose rate which indicates lower shielding is reported by sand UHPdC which 2.06 $\times 10^{-7}$ µsv/hour/source. This is followed by barite and magnetite UHPdC at 9.99 $\times 10^{-8}$ and 7.09 $\times 10^{-8}$ µsv/hour/source respectively. These findings validate the experimental work on gamma ray attenuation of UHPdCs based on the ranking of gamma ray shielding property. Table 5 summarizes the effective dose of simulation which correlates with density of UHPdC that validates the findings of experimental work.

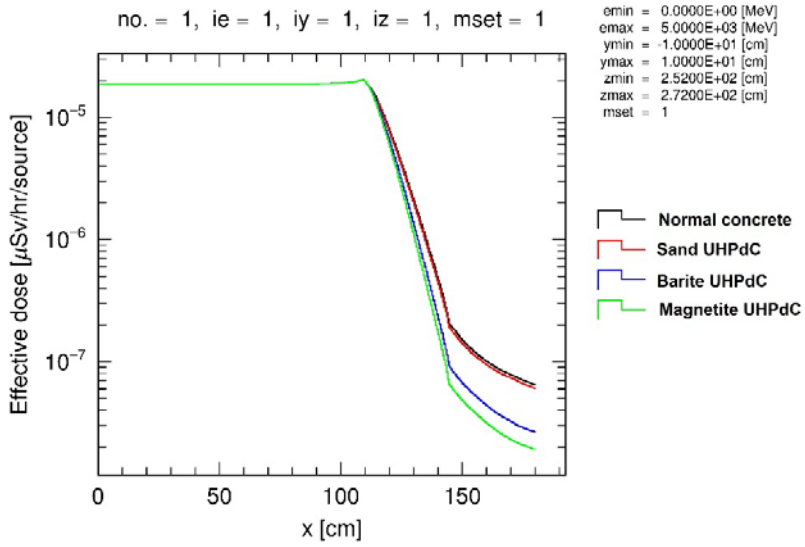

Figure 5: Simulated effective dose of gamma ray for dry cask of normal concrete and optimized UHPdC

Table 5: Summary of density, effective dose and linear attenuation coefficient of all UHPdCs

Type of UHPdC	**Density (kg/m^3)**	**Effective dose (µsv/hours/source)**	**Linear attenuation coefficient from experiment (cm^{-1})**
Sand UHPdC	2374	2.06×10^{-7}	0.1663
Barite UHPdC	2776	9.99×10^{-8}	0.1957
Magnetite UHPdC	2991	7.09×10^{-8}	0.1972

Simulated flux value due to neutron radiation is shown in Figure 6 where all UHPdC cask are able to reduce the flux to less than 10^{-5} cm^{-2}/source for region beyond the wall. The highest shielding of neutron which is indicated by blue colour is shown by Magnetite UHPdC and this is followed with sand and barite UHPdC. Based on the changes of colour from teal to blue near the surface of the cask for each type of UHPdC indicates sudden reduction of flux which shows effectiveness of shielding by UHPdC material. Effective dose result in magnetite UHPdC cask also demonstrate the superiority of neutron shielding in magnetite UHPdC compared to others (Figure 7a). Value of effective dose tracked at beyond wall which is at distance of 114 cm is the lowest in magnetite UHPdC. This finding is congruent with experimental work as magnetite UHPdC posses the highest neutron shielding property.

Further analysis on flux tracked on the outer face of cask wall shows low shielding of neutron by barite UHPdC (Figure 7b). Comparison between initial flux and flux tracked at outer wall of barite UHPdC cask indicates that high amount of neutron with high energy passed through the wall that indicates lower neutron shielding. Furthermore, low amount of lower enegy flux detected at outer wall of barite UHPdC cask indicates that less

high energy flux being attenuated to lower energy level. This is further indication of lower neutron shielding in barite UHPdC.

Overall, highest shielding of neutron shown in simulation by magnetite UHPdC validates the finding in expriment work. Discrepancy shown between result of barite UHPdC cask storage and the experimental work is due to difference level neutron's energy distribution. Experimental work employs AmBe source while simulated work is an alpha and neutron reaction of fissile material of spent fuel which is higher energy level. Furthermore, experimental work used helium detector for thermal neutrons only while the all particles are tracked in simulation. However, the difference is small and the results are still comparable. The low in neutron shielding of barite is also highlighted by a study which reported that resence of barite reduced the amount of neutron moderator in concrete hence lowering the neutron shielding based on the calculated neutron shielding coefficient [38][41]. Overall, the findings of simulation show the impact of element combination on neutron shielding which Fe and B elements combination produces positive result on neutron shielding property.

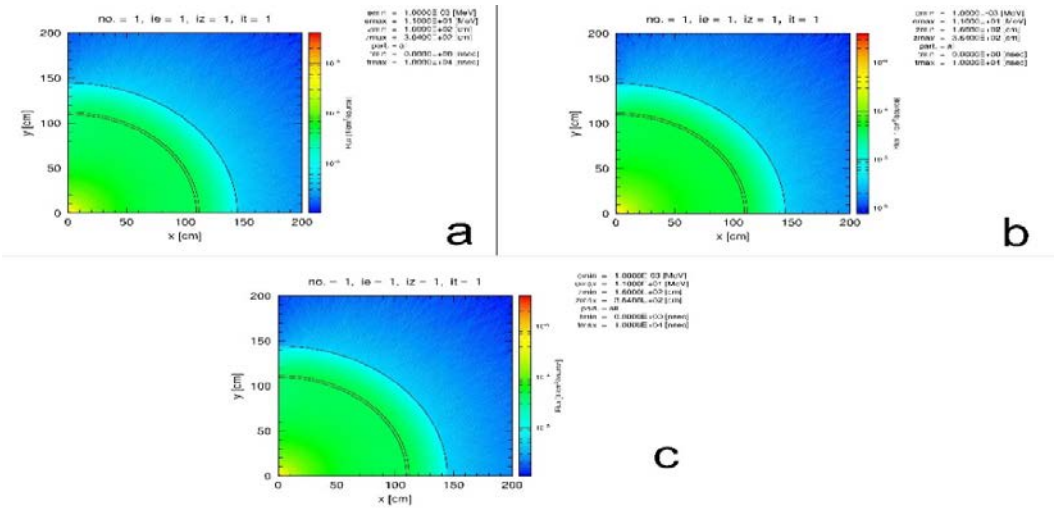

Figure 6: Simulated flux from neutron radiation of dry cask storage using a. sand UHPdC, b. barite UHPdC and c. magnetite UHPdC

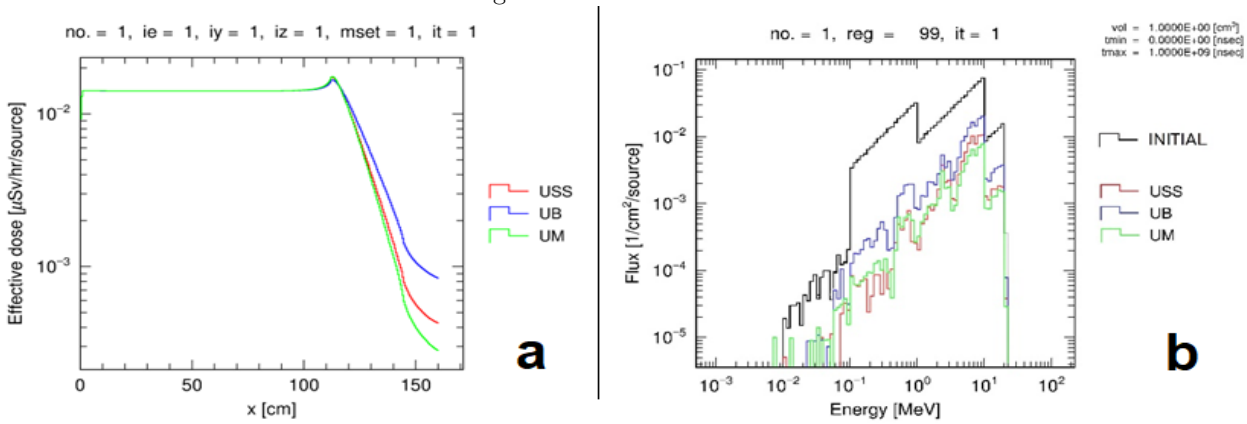

Figure 7: Simulated a) effective dose and b) flux value of initial flux (INITIAL) and flux value at the outer face of dry cask of sand UHPdC (USS), barite UHPdC (UB) and magnetite UHPdC (UM).

CONCLUSION

This study aimed to simulate the performance of UHPdC in terms of mechanical and radiation shielding properties using ANSYS and PHITS. Based on the results and analysis of data, the following conclusions are drawn:

1. Mechanical properties of UHPdC relies heavily on the aggregate type which is validated with simulation data.
2. Simulated dry cask storage of UHPdC shows viability of all types of UHPdC as cask for storing spent fuel cell.
3. Gamma radiation shielding of UHPdC is largely influenced by density as magnetite UHPdC recorded the highest value based on exposure to Cs-137 and Co-60.
4. Neutron shielding based on AmBe source shows largest value recorded by magnetite UHPdC due to Fe element in the aggregate. Combination of element with large scattering cross section, neutron moderator and neutron absorber produced UHPdC with higher neutron radiation shielding property.
5. Overall, magnetite UHPdC shows overall practical mechanical strength and highest radiation shielding property.

DECLARATION OF COMPETING INTEREST

The authors would like to declare that there is no known competing financial interest and conflicting personal relationships that could have emerged to have effect on the work reported in this manuscript.

ACKNOWLEDGMENT

The authors gratefully acknowledge the financial support by the University Putra Malaysia, Malaysia Nuclear Agency and Dura Technology Sdn. Bhd.

REFERENCES

[1] N. A. Nordin, Z. Laili, and K. Samuding, "Persoalan tentang sinaran dan teknologi nuklear," *i-Nuklear*, 2019.

[2] B. Baharuddin, H. Adnan, N. Mat Isa, N. P. bin M. Hasan, and S. S. Mat Sali, "MENANGANI COVID-19 : SUMBANGAN TEKNOLOGI NUKLEAR Sejarah Peranan," *i-Nuklear*, vol. 3, 2020.

[3] G. R. CHOPPIN, J.-O. LILJENZIN, and J. RYDBERG, "Absorption of Nuclear Radiation," *Radiochem. Nucl. Chem.*, pp. 123–165, 2002, doi: 10.1016/b978-075067463-8/50006-6.

[4] D. J. Naus, C. B. Oland, B. Ellingwood, Y. Mori, and E. G. Arndt, "Aging of concrete containment structures in nuclear power plants," p. 71, 1992, [Online]. Available: http://inis.iaea.org/search/search.aspx?orig_q=RN:23071987.

[5] Centers for Disease Control and Prevention, "CDC Radiation Emergencies | Radioactive Contamination and Radiation Exposure." https://www.cdc.gov/nceh/radiation/emergencies/contamination.htm.

[6] A. S. Ouda, "Development of high-performance heavy density concrete using different aggregates for gamma-ray shielding," *Prog. Nucl. Energy*, vol. 79, pp. 48–55, 2015, doi: 10.1016/j.pnucene.2014.11.009.

[7] N. M. Azreen *et al.*, "Simulation of ultra-high-performance concrete mixed with hematite and barite aggregates using Monte Carlo for dry cask storage," *Constr. Build. Mater.*, vol. 263, p. 120161, 2020, doi: 10.1016/j.conbuildmat.2020.120161.

[8] O. Lotfi-Omran, A. Sadrmomtazi, and I. M. Nikbin, "A comprehensive study on the effect of water to cement ratio on the mechanical and radiation shielding properties of heavyweight concrete," *Constr. Build. Mater.*, vol. 229, 2019, doi: 10.1016/j.conbuildmat.2019.116905.

[9] T. Shams, M. Eftekhar, and A. Shirani, "Investigation of gamma radiation attenuation in heavy concrete shields containing hematite and barite aggregates in multi-layered and mixed forms," *Constr. Build. Mater.*, vol. 182, pp. 35–42, 2018, doi: 10.1016/j.conbuildmat.2018.06.032.

[10] K. Zalegowski, T. Piotrowski, A. Garbacz, and G. Adamczewski, "Relation between microstructure, technical properties and neutron radiation shielding efficiency of concrete," *Constr. Build. Mater.*, vol. 235, 2020, doi: 10.1016/j.conbuildmat.2019.117389.

[11] Demir, M. Gümüş, and H. S. Gökçe, "Gamma ray and neutron shielding characteristics of polypropylene fiber-reinforced heavyweight concrete exposed to high temperatures," *Constr. Build. Mater.*, vol. 257, 2020, doi: 10.1016/j.conbuildmat.2020.119596.

[12] D. E. Tobbala, "Effect of Nano-ferrite addition on mechanical properties and gamma ray attenuation coefficient of steel fiber reinforced heavy weight concrete," *Constr. Build. Mater.*, vol. 207, pp. 48–58, 2019, doi: 10.1016/j.conbuildmat.2019.02.099.

[13] A. Mesbahi, G. Alizadeh, G. Seyed-Oskoee, and A. A. Azarpeyvand, "A new barite-colemanite concrete with lower neutron production in radiation therapy bunkers," *Ann. Nucl. Energy*, vol. 51, pp. 107–111, 2013, doi: 10.1016/j.anucene.2012.07.039.

[14] D. Mostofinejad, M. Reisi, and A. Shirani, "Mix design effective parameters on γ-ray attenuation coefficient and strength of normal and heavyweight concrete," *Constr. Build. Mater.*, vol. 28, no. 1, pp. 224–229, 2012, doi: 10.1016/j.conbuildmat.2011.08.043.

[15] K. Saidani, L. Ajam, and M. Ben Ouezdou, "Barite powder as sand substitution in concrete: Effect on some mechanical properties," *Constr. Build. Mater.*, vol. 95, pp. 287–295, 2015, doi: 10.1016/j.conbuildmat.2015.07.140.

[16] S. H. Al-Tersawy, R. A. El-Sadany, and H. E. M. Sallam, "Experimental gamma-ray attenuation and theoretical optimization of barite concrete mixtures with nanomaterials against neutrons and gamma rays," *Constr. Build. Mater.*, vol. 289, p. 123190, 2021, doi: 10.1016/j.conbuildmat.2021.123190.

[17] H. Binici, O. Aksogan, A. H. Sevinc, and A. Kucukonder, "Mechanical and radioactivity shielding performances of mortars made with colemanite, barite, ground basaltic pumice and ground blast furnace slag," *Constr. Build. Mater.*, vol. 50, pp. 177–183, 2014, doi: 10.1016/j.conbuildmat.2013.09.033.

[18] S. Yousef, M. AlNassar, B. Naoom, S. Alhajali, and M. H. Kharita, "Heat effect on the shielding and strength properties of some local concretes," *Prog. Nucl. Energy*, vol. 50, no. 1, pp. 22–26, 2008, doi: 10.1016/j.pnucene.2007.10.003.

[19] E. Horszczaruk and P. Brzozowski, "Investigation of gamma ray shielding efficiency and physicomechanical performances of heavyweight concrete subjected to high temperature," *Constr. Build. Mater.*, vol. 195, pp. 574–582, 2019, doi: 10.1016/j.conbuildmat.2018.09.113.

[20] F. Zhang *et al.*, "Experimental study of CFDST columns infilled with UHPC under close-range blast loading," *Int. J. Impact Eng.*, vol. 93, pp. 184–195, 2016, doi: 10.1016/j.ijimpeng.2016.01.011.

[21] P. Máca, R. Sovják, and P. Konvalinka, "Mix design of UHPFRC and its response to projectile impact," *Int. J. Impact Eng.*, vol. 63, pp. 158–163, 2014, doi: 10.1016/j.ijimpeng.2013.08.003.

[22] J. Zhu, C. Sun, Z. Qian, and J. Chen, "The spalling strength of ultra-fiber reinforced cement mortar," *Eng. Fail. Anal.*, vol. 18, no. 7, pp. 1808–1817, 2011, doi: 10.1016/j.engfailanal.2011.05.001.

[23] D. Zhang, Y. Zhang, A. Dasari, K. H. Tan, and Y. Weng, "Effect of spatial distribution of polymer fibers on preventing spalling of UHPC at high temperatures," *Cem. Concr. Res.*, vol. 140, no. November 2020, 2021, doi: 10.1016/j.cemconres.2020.106281.

[24] D. Zhang and K. H. Tan, "Effect of various polymer fibers on spalling mitigation of ultra-high performance concrete at high temperature," *Cem. Concr. Compos.*, vol. 114, no. September, pp. 1–9, 2020, doi: 10.1016/j.cemconcomp.2020.103815.

[25] N. M. Azreen, R. S. M. Rashid, M. Haniza, Y. L. Voo, and Y. H. Mugahed Amran, "Radiation shielding of ultra-high-performance concrete with silica sand, amang and lead glass," *Constr. Build. Mater.*, vol. 172, pp. 370–377, 2018, doi: 10.1016/j.conbuildmat.2018.03.243.

[26] M. U. Khan, S. Ahmad, A. A. Naqvi, and H. J. Al-Gahtani, "Shielding performance of heavy-weight ultra-high-performance concrete against nuclear radiation," *Prog. Nucl. Energy*, vol. 130, no. October, p. 103550, Dec. 2020, doi: 10.1016/j.pnucene.2020.103550.

[27] R. S. M. Rashid *et al.*, "Effect of elevated temperature to radiation shielding of ultra-high performance concrete with silica sand or magnetite," *Constr. Build. Mater.*, vol. 262, p. 120567, 2020, doi: 10.1016/j.conbuildmat.2020.120567.

[28] S. M. Rasoul Abdar Esfahani, S. A. Zareei, M. Madhkhan, F. Ameri, J. Rashidiani, and R. A. Taheri, "Mechanical and gamma-ray shielding properties and environmental benefits of concrete incorporating GGBFS and copper slag," *J. Build. Eng.*, vol. 33, no. February 2020, 2021, doi: 10.1016/j.jobe.2020.101615.

[29] A. El-Sayed Abdo, M. A. M. Ali, and M. R. Ismail, "Influence of magnetite and boron carbide on radiation attenuation of cement-fiber/composite," *Ann. Nucl. Energy*, vol. 30, no. 4, pp. 391–403, 2003, doi: 10.1016/S0306-4549(02)00074-9.

[30] N. Singh, K. J. Singh, K. Singh, and H. Singh, "Gamma-ray attenuation studies of PbO-BaO-B2O3 glass system," *Radiat. Meas.*, vol. 41, no. 1, pp. 84–88, 2006, doi: 10.1016/j.radmeas.2004.09.009.

[31] M. H. Kharita, S. Yousef, and M. AlNassar, "The effect of the initial water to cement ratio on shielding properties of ordinary concrete," *Prog. Nucl. Energy*, vol. 52, no. 5, pp. 491–493, Jul. 2010, doi: 10.1016/j.pnucene.2009.11.005.

[32] J. Castro, R. P. Spragg, P. Compare, and W. J. Weiss, "Portland cement concrete pavement permeability perfromance," *Fhwa/in/Jtrp-2010/29, Spr-3093*, no. November, 2010.

[33] J. Ko, J. Park, I. Jung, G. Lee, C. Baeg, and T. Kim, "SHIELDING ANALYSIS OF DUAL PURPOSE CASKS FOR SPENT NUCLEAR FUEL UNDER NORMAL STORAGE CONDITIONS," *Nucl. Eng. Technol.*, vol. 46, no. 4, pp. 547–556, 2014, doi: 10.5516/NET.08.2013.039.

[34] S. L. Yang, S. G. Millard, M. N. Soutsos, S. J. Barnett, and T. T. Le, "Influence of aggregate and curing regime on the mechanical properties of ultra-high performance fibre reinforced concrete (UHPFRC)," *Constr. Build. Mater.*, vol. 23, no. 6, pp. 2291–2298, 2009, doi: 10.1016/j.conbuildmat.2008.11.012.

[35] M. A. González-Ortega, S. H. P. Cavalaro, and A. Aguado, "Influence of barite aggregate friability on mixing process and mechanical properties of concrete," *Constr. Build. Mater.*, vol. 74, pp. 169–175, 2015, doi: 10.1016/j.conbuildmat.2014.10.040.

[36] E. Horszczaruk, P. Sikora, and P. Zaporowski, "Mechanical properties of shielding concrete with magnetite aggregate subjected to high temperature," *Procedia Eng.*, vol. 108, pp. 39–46, 2015, doi: 10.1016/j.proeng.2015.06.117.

[37] K. H. Yang, J. S. Mun, and H. J. Shim, "Shrinkage of heavyweight magnetite concrete with and without fly ash," *Constr. Build. Mater.*, vol. 47, pp. 56–65, 2013, doi: 10.1016/j.conbuildmat.2013.05.034.

[38] I. Akkurt and A. M. El-Khayatt, "The effect of barite proportion on neutron and gamma-ray shielding," *Ann. Nucl. Energy*, vol. 51, pp. 5–9, 2013, doi: 10.1016/j.anucene.2012.08.026.

[39] F. A. R. Schmidt, "ATTENUATION PROPERTIES OF CONCRETE FOR SHIELDING OF NEUTRONS OF ENERGY LESS THAN 15 MeV.," United States, 1970. doi: 10.2172/4115490.

[40] M. G. El-samrah, M. A. A. Zamora, D. R. Novog, and S. E. Chidiac, "Progress in Nuclear Energy Radiation shielding properties of modified concrete mixes and their suitability in dry storage cask," *Prog. Nucl. Energy*, vol. 148, no. July 2021, p. 104195, 2022, doi: 10.1016/j.pnucene.2022.104195.

[41] H. S. Gökçe, Ç. Yalçınkaya, and M. Tuyan, "Optimization of reactive powder concrete by means of barite aggregate for both neutrons and gamma rays," *Constr. Build. Mater.*, vol. 189, pp. 470–477, 2018, doi: 10.1016/j.conbuildmat.2018.09.022.